MANTIS®
MANTIS DEPOSITION LTD

APPLICATION NOTE

OPPORTUNITIES FOR AND EXAMPLES OF SCALE UP FOR SILVER NANOPARTICLE DEPOSITION

INTRODUCTION

Silver Nanoparticles (Ag NPs) have been proven to add functionality to a range of applications across many different nanotechnology sectors, from solar energy, through medical and gas sensing to food packaging.

In the solar industry the inclusion of Ag NPs has shown a 22.7% increase in efficiency of polycrystalline Si solar cells due to the enhanced surface plasmon resonance (SPR) effect [1]. Precise control over the NP size and shape is required to yield control over the SPR frequency and intensity [2], [3]. Measurement of the SPR frequency for Ag NPs prepared by NIL (NanoImprint Lithography) showed a shift of 160nm to longer wavelength with increasing NP diameter from 10 to 40nm. The normalized extinction is shown in Figure 1 for 10nm, 20nm, 30nm, and 40nm Ag NPs [4].

Control over the shape of the Ag NP has also been shown to affect the UV-visible absorption spectrum of the NPs [5] [6]. Coupled Ag NPs show benefits to SPR gas and chemical sensors. The shift of the plasmon resonance to longer wavelength relative to the single Ag NP SPR yields enhanced sensitivity to changes in sensing medium [7].

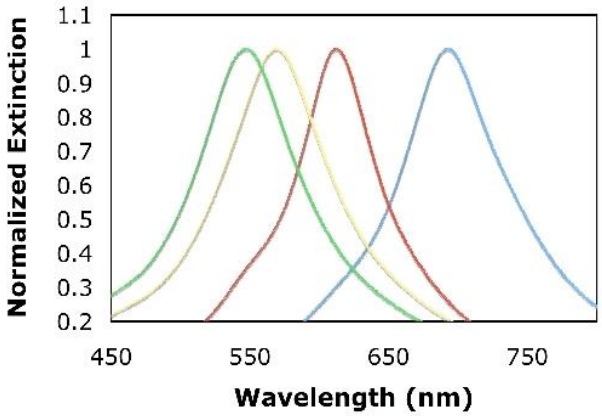

Figure1. Normalized extinction for 10, 20, 30, 40nm NPs [4]

The antimicrobial properties of Ag NPs are already being used in commercial products such as odour controlling socks (NanoSilver®), home appliances (SAMSUNG Silver Nano® refrigerator), wound dressing (ACTICOAT®) and also in the food industry [MicroSilver BG® Tec]. The presence of Ag NP coated braids significantly reduced the room temperature growth of yeasts, coliform bacteria, Escherichia coli, and Staphylococcus aureus moulds in cow's milk while maintaining the Ag NP count in the milk below safe limits for

human consumption [8]. The shape of the Ag NP can also affect the bactericidal properties of the NP, due to the varying chemical reactivity of different crystal orientations [9].

NANOPARTICLE DEPOSITION

The Mantis Deposition NanoGen50 terminated gas condensation (TGC) method allows tight control of the nanoparticles size and structure [10]. Furthermore, as the control parameters of the NanoGen50 are altered by the user, it is possible to monitor and filter the nanoparticles size in situ by using the Mantis Deposition MesoQ, a high throughput quadrupole mass filter. The high charging ratios of the NPs allow further control over the porosity of the film deposited on the substrate.

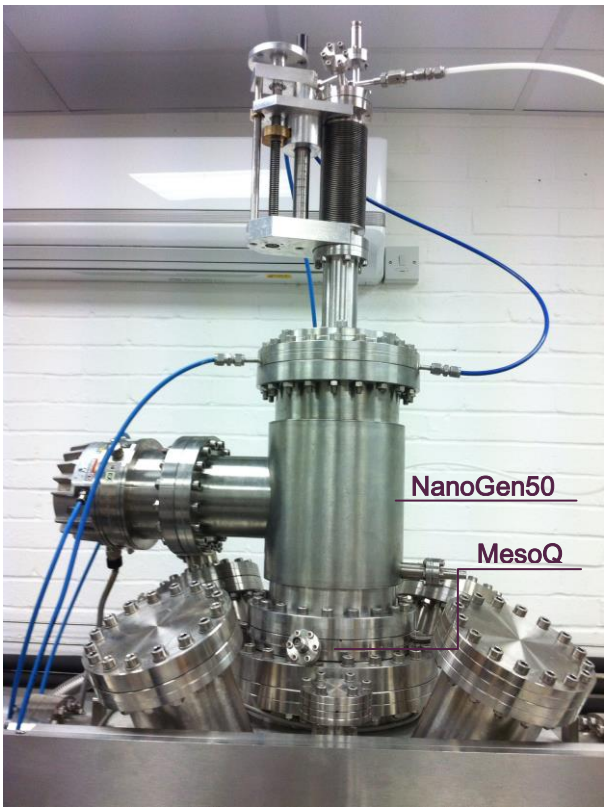

Figure 2. NanoGen50 and MesoQ

The NanoGen50 offers a process which generates NPs which are inherently purer and with far superior control over size and shape compared to other techniques, such as chemical synthesis and self-organised nanoparticles formed by thermal evaporation.

Historically chemical synthesis has offered the only method of producing large volumes of NPs (gram quantities). Our nanoparticle source now offers the superior size and shape control of Ag NPS with the added opportunity to scale up to mass production. Here we present results which show that the NanoGen50 can be used in continuous operation as a mass production tool to rival other NP processes.

Silver Nanoparticles (NP) were produced using the Mantis NanoGen50. The silver target was sputtered using a DC magnetron at a power of ~ 45W. Ar process gas was fed directly into the aggregation zone to yield a process pressure of ~ 10^{-3} mbar. The MesoQ mass filter was connected in line with the nanoparticle generator and was set up to detect a distribution of nanoparticles generated in Nanogen50.

The stable Ag NP deposition was performed using two different magnet sets, set A and set B. Set A is a strong type 2 magnet set which yields 100% charging ratio (of negatively charged to uncharged NPs) of Ag NPs. This is important for applications where the manipulation of the NPs (mass filtering or acceleration) is required. Magnet set B yields a slightly lower charging ratio (80-90%) but a higher target usage. More importantly, higher deposition rates (up to 10x higher than for set A) are achievable which is important for applications where high loading is required. Figure 3 shows the shape of the magnetic field for sets A and B.

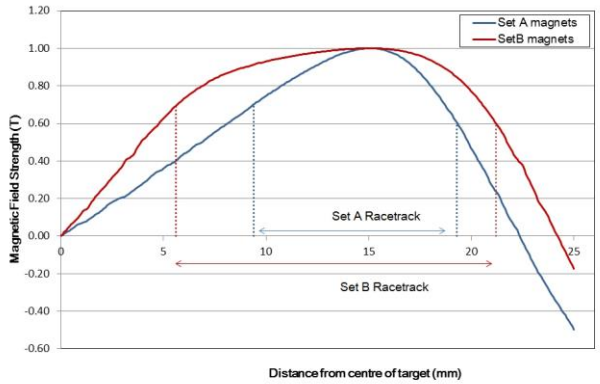

Figure 3. Magnetic field modelled at the surface of Ag target for set A and set B magnets

MAGNET SET A

The continuous operation mass spectrum as measured by the MesoQ is plotted in Figure 4 for the Ag NP with Set A magnets.

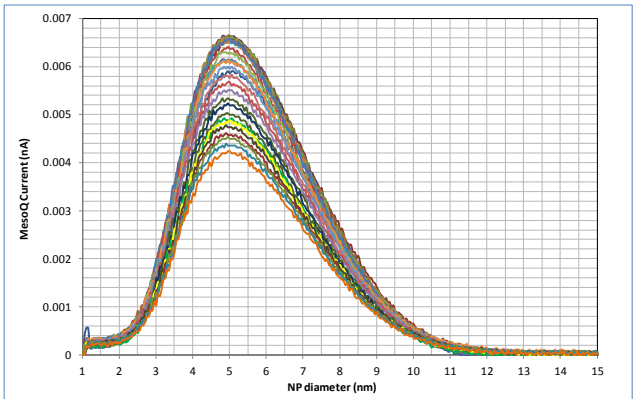

Figure 4. Ag NP MesoQ spectra with set A magnets measured over 1 hour

The NanoGen50 conditions were fixed for gas flow, aggregation length and magnetron current. Tight control over the Ag NP size to within ±0.05nm is demonstrated over the 1 hour period. When applied to plasmonics for example, such tight control equates to less than 1.5meV shift in plasmon resonance frequency. The drop in MesoQ signal over time is associated with a drop in the plasma voltage at constant current due to erosion of the target. This can be partially offset by running the process in constant power mode.

MAGNET SET B

The use of Magnet set B offers an Ag NP process with enhanced deposition rates due to the wider race track. The MesoQ spectrum for Ag NP process using Set B magnets is shown in Figure 5, where the expected higher signal than for set A magnets can be seen.

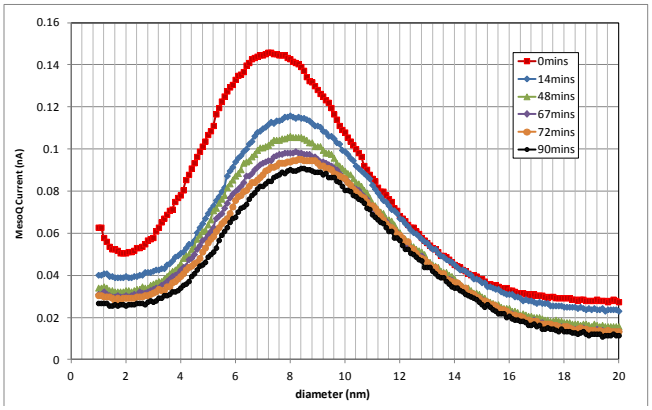

Figure 5. MesoQ spectra for continuous Ag NP process with set B magnets

It appears that the MesoQ spectrum drifts to larger NP sizes and lower intensities with time. This may be explained by a drop in plasma voltage, which in turn, affects the plasma temperature and nucleation rate of the Ag NPs.

A stable Ag NP process may be obtained for the Set B magnets by the controlled injection of He into the aggregation zone. Figure 6 shows the nanoparticle distribution obtained when the He flow is adjusted between 1-5sccm to maintain a stable Ag NP process over a 90 minute period. The NP size is controlled to within ± 0.05nm, which is the same accuracy as offered by the set A magnets. The introduction of He into the NanoGen50 chamber does not affect the

sputtering yield at the Ag target surface, but instead cools the plasma by removing heat from the aggregation zone and thus, helps to maintain a stable nucleation rate for Ag NPs.

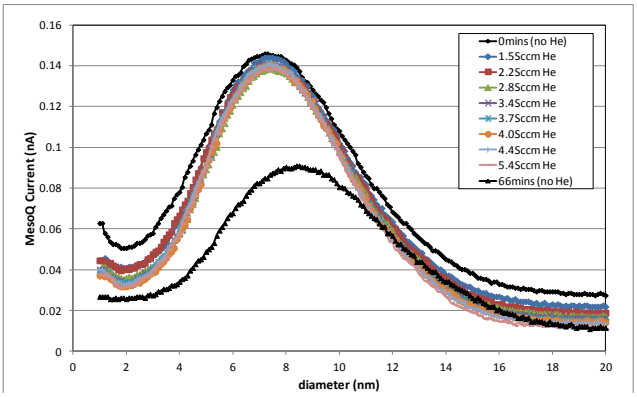

Figure 6. He flow control of Ag NP process for set B magnets

Monitoring of the MesoQ mass spectrum and adjustment of the He flow may be controlled using the Mantis TITANIUM software to provide an automated and stable Ag NP process with high deposition rates and fine control over the Ag NP size.

CONCLUSIONS

The Mantis NanoGen50 and MesoQ mass filter offer a stable process for generating Ag NP using the terminated gas condensation method. Two different magnet configurations have been reported, both exhibiting different advantages for a mass production process. The stronger set A magnets yield a very stable NP size distribution but inefficient use of the target material. The magnet set B yields higher deposition rates and high target usage efficiency, which is especially important for precious metals such as silver. A stable NP generation may be achieved with the use of He in the aggregation zone.

Using the same techniques as for silver, a nanoparticle production process can also be extended to other materials. Please contact us for further details at sales@mantisdeposition.com.

REFERENCES

[1] Haila M. Al Dosari, Ahmad I. Ayesh; J. Appl. Phys. 2013, 114:054305.

[2] J. Scholl, A Koh, J. Dionne; Nature, 2012, 483 421-427.

[3] Rita Najjar, Salim Boutami, Cyril Cayron, Nathalie Baclet, Viviane Muffato, Pierre Labeye, Alistair Kean, Srinivas Saranu, Etienne Quesnel; Advanced Mat Res 2011, 324:113-118.

[4] C Chen; J. Young Investigators, 2007.

[5] Gracia-Pinilla MA, Pérez-Tijerina E, García JA, Fernández-Navarro C, Tlahuice-Flores A, Mejía-Rosales S, Montejano-Carrizales JM, José-Yacamán M; J. Phys. Chem. C. 2008, 112:13492.

[6] V Amendola, O M Bkr; Plasmonics. 2010, 5, 85-97.

[7] Shiliang Wang, David B. Pedersen; J. Phys. Chem. C. 2010, 114:2861–2866.

[8] Yildiz N, Pala A; J Dairy Sci. 2012, 95:1119-1127.

[9] T.V. Duncan; J Colloid. Int. Sci. 2001, 10, 1016.

[10] Gracia-Pinilla MA, Ferrer D, Mejía-Rosales S, Pérez-Tijerina E; Nanoscale Res. Lett. 2009, 4:896-902.